Hindawi Publishing Corporation
Advances in High Energy Physics
Volume 2013, Article ID 143184, 11 pages
http://dx.doi.org/10.1155/2013/143184

Research Article

Cross Sections of Charged Current Neutrino Scattering off ^{132}Xe for the Supernova Detection

P. C. Divari

Department of Physical Sciences and Applications, Hellenic Army Academy, Vari, Attica 16673, Greece

Correspondence should be addressed to P. C. Divari; pdivari@gmail.com

Received 28 November 2012; Accepted 19 January 2013

Academic Editor: Joseph Formaggio

The total cross sections as well as the neutrino event rates are calculated in the charged current neutrino and antineutrino scattering off ^{132}Xe isotope at neutrino energies $E_\upsilon < 100$ MeV. Transitions to excited nuclear states are calculated in the framework of quasiparticle random-phase approximation. The contributions from different multipoles are shown for various neutrino energies. Flux-averaged cross sections are obtained by convolving the cross sections with a two-parameter Fermi-Dirac distribution. The flux-averaged cross sections are also calculated using terrestrial neutrino sources based on conventional sources (muon decay at rest) or on low-energy beta-beams.

1. Introduction

The detection of neutrinos and their properties is one of the top priorities of modern nuclear and particle physics as well as astrophysics. Among the probes which involve neutrinos, the neutrino-nucleus reactions possess a prominent position. Detailed predictions of neutrino-nucleus cross sections (NNCS) are crucial to detect or distinguish neutrinos of different flavor and explore the basic structure of the weak interactions [1–14]. Mured cross sections for neutrino-nucleus scattering at neutrino energies which are relevant for supernova neutrinos are available in only a few cases, that is, for ^{56}Fe [15], ^{12}C [15, 16], and the deuteron [17]. The use of microscopic nuclear structure models is therefore essential, for a quantitative description of neutrino-nucleus reactions. These include the nuclear shell model [18, 19], the random-phase approximation (RPA), relativistic RPA [20, 21], continuum RPA (CRPA) [22], quasiparticle RPA (QRPA) [23–26], projected quasiparticle RPA (PQRPA) [27], hybrid models of CRPA, the shell model [28, 29], and the Fermi gas model [30]. The shell model provides a very accurate description of ground-state wave functions. The description of high-lying excitations, however, necessitates the use of large-model spaces, and this often leads to computational difficulties, making the approach applicable essentially only to light- and medium-mass nuclei. Therefore, for, systematic studies of weak interaction rates for relevant heavy nuclei of mass number around $A = 128$–132, microscopic calculations must be performed using models based on the RPA [23, 25].

The signature of supernova neutrino interaction taking place in various detectors is the observation of electrons, positrons, photons, and other particles which are produced through the charged and neutral current interactions. Two processes that contribute to the total event rates in the detectors are the charged current (CC) reactions

$$\begin{aligned} \nu_e + {}_Z X_N &\longrightarrow {}_{Z+1}X^*_{N-1} + e^-, \\ \overline{\nu}_e + {}_Z X_N &\longrightarrow {}_{Z-1}X^*_{N+1} + e^+ \end{aligned} \tag{1}$$

and the neutral current (NC) reactions

$$\nu_x\,(\overline{\nu}_x) + {}_Z X_N \longrightarrow \nu_x\,(\overline{\nu}_x) + {}_Z X^*_N, \quad x = e, \mu, \tau. \tag{2}$$

The neutrinos ν_x (or antineutrinos $\overline{\nu}_x$) with $x = \mu, \tau$ do not have sufficient energy to produce corresponding leptons in charged current reactions and interact only through neutral current interactions and therefore have a higher-average energy than ν_e and $\overline{\nu}_e$, which interact through charged current as well as neutral current interactions. Numerical simulations give the following values of average energy for the different neutrino flavors, that is, $\langle E_{\nu_e} \rangle \sim$ 10-11 MeV, $\langle E_{\overline{\nu}_e} \rangle \sim$ 15-16 MeV, and $\langle E_{\nu_x} \rangle \sim$ 23–25 MeV, and are consistent with

the supernova neutrino spectrum given by a Fermi-Dirac distribution [31, 32]:

$$\phi\left(E_\nu\right) = \frac{N_2\left(\alpha\right)}{T^3}\frac{E_\nu^2}{1+\exp\left[\left(E_\nu/T\right)-\alpha\right]}, \tag{3}$$

where T is the neutrino temperature, α is a degeneracy parameter taken to be either 0 or 3. $N_2(\alpha)$ denotes the normalization factor depending on α given from

$$N_k\left(\alpha\right) = \left(\int_0^\infty \frac{x^k}{1+e^{x-\alpha}}dx\right)^{-1}, \tag{4}$$

for $k = 2$. Following [33], the average neutrino energy $\langle E_\nu\rangle$ can be written in terms of the functions of (4) as

$$\left\langle E_\nu\right\rangle = \frac{N_2\left(\alpha\right)}{N_3\left(\alpha\right)}T. \tag{5}$$

Most calculations of neutrino-nucleus cross sections have been taken the value $\alpha = 0$. However, in astrophysical applications, it might be important to perform studies of reaction rates for different values of α depending on the simulation performed and on the specific supernova phase considered [29, 34]. In our study, the value $\alpha = 3$ has also been used. The average energy values for the various neutrino species imply that for $\alpha = 0(3)$, the values of temperature T are 3.5 MeV (2.75 MeV) for ν_e, 5 MeV (4 MeV) for $\overline{\nu}_e$, and 8 MeV (6 MeV) for ν_x ($x = \mu, \tau, \overline{\mu}, \overline{\tau}$). The recent theoretical studies predict a smaller value of temperature for ν_x which is closer to $\overline{\nu}_e$ [34–37].

Systematic neutrino-nucleus interaction measurements could be an ideal tool to explore the weak nuclear response. At present, new experiments on various nuclei are being proposed with a new facility using muon decay at rest [38]. Another possibility could be offered by beta-beams. This is a new method to produce pure and well-known electron neutrino beams, exploiting the beta-decay of boosted radioactive ions [39]. The idea of establishing a low-energy beta-beam facility has been first proposed in [40] and discussed in nuclear structure studies, core-collapse supernova physics, and the study of fundamental interactions [40–49].

A detector whose active target consists of the noble liquid Xenon can offer unique detection capabilities in the field of neutrino physics [47, 50] as well as the ability to detect very low-energy signals in the context of dark matter searches [51, 52]. The new concept of a spherical TPC detector, filled with high-pressure Xenon, has also been proposed as a device able to detect low-energy neutrinos as those coming from a galactic supernova. In particular, a TPC detector can be used to observe coherent NC as well as CC neutrino-nucleus scattering [37, 53–58].

In this paper, we present microscopic calculations of the CC

$$\nu_e\left(\overline{\nu}_e\right) + {}^{132}\mathrm{Xe} \longrightarrow {}^{132}\mathrm{Cs}^*\left({}^{132}\mathrm{I}^*\right) + e^-\left(e^+\right) \tag{6}$$

reaction cross sections. The corresponding-reduced matrix elements in the low- and intermediate-neutrino energy range have been calculated in the framework of quasiparticle random-phase approximation (QRPA). We present the total neutrino-nucleus cross sections as well as the contribution of the various multipoles and discuss how their importance evolves, as a function of neutrino energy. A comparison between the CC cross sections and those involved by the coherent NC ones [37, 55] is also presented. Finally, we give the flux-averaged cross sections associated to the Fermi-Dirac distribution as well as to distributions based on terrestrial neutrino sources such as the low-energy beta-beams or to conventional sources (muon decay at rest).

2. The Formalism for Neutrino-Nucleus Cross Sections Calculations

Let us consider a neutral or charged current neutrino-nucleus interaction in which a low- or intermediate-energy neutrino (or antineutrino) is scattered inelastically from a nucleus (A, Z). The initial nucleus is assumed to be spherically symmetric having ground state a $|J^\pi\rangle = |0^+_{\mathrm{gs}}\rangle$ state.

The corresponding standard model effective Hamiltonian of the current-current interaction can be written as

$$\mathscr{H} = \frac{Ga^{\mathrm{CC,NC}}}{\sqrt{2}}j_\mu\left(\mathbf{x}\right)J^\mu\left(\mathbf{x}\right), \tag{7}$$

where $G = 1.1664\times10^{-5}\,\mathrm{GeV}^{-2}$ is the Fermi weak coupling constant, $a^{\mathrm{CC}} = \cos\theta_c$ for charged current reaction, and $a^{\mathrm{NC}} = 1$ for neutral current reaction. j_μ and J^μ denote the leptonic and hadronic currents, respectively. According to V-A theory, the leptonic current takes the form

$$j_\mu = \overline{\psi}_{\nu_\ell}\left(x\right)\gamma_\mu\left(1-\gamma_5\right)\psi_{\nu_\ell}\left(x\right), \tag{8}$$

where ψ_{ν_ℓ} are the neutrino/antineutrino spinors.

From a nuclear physics point of view, only the hadronic current is important. The structure for neutral current (NC) and charged current (CC) processes of both vector and axial-vector components (neglecting the pseudoscalar contributions) is written as

$$J_\mu^{\mathrm{CC,NC}} = \overline{\psi}_N\left[F_1^{\mathrm{CC,NC}}\left(q^2\right)\gamma_\mu + F_2^{\mathrm{CC,NC}}\left(q^2\right)\frac{i\sigma_{\mu\nu}q^\nu}{2M} + F_A^{\mathrm{CC,NC}}\left(q^2\right)\gamma_\mu\gamma_5\right]\psi_N, \tag{9}$$

where M stands for the nucleon mass, and ψ_N denote the nucleon spinors. The form factors $F_{1,2}^{\mathrm{CC}}(q^2)$ and $F_A^{\mathrm{CC}}(q^2)$ are defined as

$$F_{1,2}^{\mathrm{CC}}\left(q^2\right) = F_{1,2}^{\mathrm{p}}\left(q^2\right) - F_{1,2}^{\mathrm{n}}\left(q^2\right),$$
$$F_A^{\mathrm{CC}}\left(q^2\right) = F_A\left(q^2\right) \tag{10}$$

and the neutral current form factors $F_{1,2}^{\mathrm{NC}}(q^2)$ and $F_A^{\mathrm{NC}}(q^2)$ as

$$\begin{aligned} F_{1,2}^{\mathrm{NC}}\left(q^2\right) &= \left(\frac{1}{2} - \sin^2\theta_W\right)\left[F_{1,2}^{\mathrm{p}}\left(q^2\right) - F_{1,2}^{\mathrm{n}}\left(q^2\right)\right]\tau_0 \\ &\quad - \sin^2\theta_W\left[F_{1,2}^{\mathrm{p}}\left(q^2\right) + F_{1,2}^{\mathrm{n}}\left(q^2\right)\right], \\ F_A^{\mathrm{NC}}\left(q^2\right) &= \frac{1}{2}F_A\left(q^2\right)\tau_0. \end{aligned} \tag{11}$$

Here, τ_0 represents the nucleon isospin operator, and θ_W is the Weinberg angle ($\sin^2\theta_W = 0.2325$). The detailed expressions of nucleonic form factors $F_{1,2}^{\mathrm{p,n}}(q^2)$ are given in [59]. The axial-vector form factor $F_A(q^2)$ is given by [60]

$$F_A = -g_A\left(1 - \frac{q^2}{M_A^2}\right)^{-2}, \tag{12}$$

where $M_A = 1.05\,\mathrm{GeV}$ is the dipole mass, and $g_A = 1.258$ is the static value (at $q = 0$) of the axial form factor.

In the convention we used in the present paper, q^2, the square of the momentum transfer, is written as

$$q^2 = q^\mu q_\mu = \omega^2 - \mathbf{q}^2 = \left(\varepsilon_i - \varepsilon_f\right)^2 - \left(\mathbf{p}_i - \mathbf{p}_f\right)^2, \tag{13}$$

where $\omega = \varepsilon_i - \varepsilon_f$ is the excitation energy of the nucleus. ε_i denotes the energy of the incoming neutrino and ε_f denotes the energy of the outgoing lepton. $\mathbf{p}_i$, $\mathbf{p}_f$ are the corresponding 3-momenta. In (11), we have not taken into account the strange quark contributions in the form factors. In the scattering reaction considered in our paper, only low-momentum transfers are involved, and the contributions from strangeness can be neglected [61].

The neutrino/antineutrino-nucleus differential cross section, after applying a multipole analysis of the weak hadronic current, is written as

$$\begin{aligned} \sigma\left(\varepsilon_i\right) &= \frac{2G^2\left(a^{\mathrm{CC,NC}}\right)^2}{2J_i + 1}\sum_f \left|\vec{p}_f\right|\varepsilon_f \\ &\quad \times \int_{-1}^{1} d\left(\cos\theta\right) F\left(\varepsilon_f, Z_f\right) \\ &\quad \times \left(\sum_{J=0}^{\infty}\sigma_{\mathrm{CL}}^J + \sum_{J=1}^{\infty}\sigma_T^J\right), \end{aligned} \tag{14}$$

where θ denotes the lepton scattering angle. The summations in (14) contain the contributions σ_{CL}^J, for the Coulomb $\widehat{\mathscr{M}}_J$ and longitudinal $\widehat{\mathscr{L}}_J$, and σ_T^J, for the transverse electric $\widehat{\mathscr{T}}_J^{\mathrm{el}}$ and magnetic $\widehat{\mathscr{T}}_J^{\mathrm{mag}}$ multipole operators [62]. These operators include both polar-vector and axial-vector weak interaction components. The contributions σ_{CL}^J and σ_T^J are written as

$$\begin{aligned} \sigma_{\mathrm{CL}}^J &= \left(1 + a\cos\theta\right)\left|\left\langle J_f \left\| \widehat{\mathscr{M}}_J(q) \right\| J_i \right\rangle\right|^2 \\ &\quad + \left(1 + a\cos\theta - 2b\sin^2\theta\right)\left|\left\langle J_f \left\| \widehat{\mathscr{L}}_J(q) \right\| J_i \right\rangle\right|^2 \\ &\quad + \left[\frac{\omega}{q}\left(1 + a\cos\theta\right) + c\right] \\ &\quad \times 2\mathfrak{Re}\left\langle J_f \left\| \widehat{\mathscr{L}}_J(q) \right\| J_i \right\rangle \left\langle J_f \left\| \widehat{\mathscr{M}}_J(q) \right\| J_i \right\rangle^*, \end{aligned} \tag{15}$$

$$\begin{aligned} \sigma_T^J &= \left(1 - a\cos\theta + b\sin^2\theta\right) \\ &\quad \times \left[\left|\left\langle J_f \left\| \widehat{\mathscr{T}}_J^{\mathrm{mag}}(q) \right\| J_i \right\rangle\right|^2 + \left|\left\langle J_f \left\| \widehat{\mathscr{T}}_J^{\mathrm{el}}(q) \right\| J_i \right\rangle\right|^2\right] \\ &\quad \mp \left[\frac{\left(\varepsilon_i + \varepsilon_f\right)}{q}\left(1 - a\cos\theta\right) - c\right] \\ &\quad \times 2\mathfrak{Re}\left\langle J_f \left\| \widehat{\mathscr{T}}_J^{\mathrm{mag}}(q) \right\| J_i \right\rangle \left\langle J_f \left\| \widehat{\mathscr{T}}_J^{\mathrm{el}}(q) \right\| J_i \right\rangle^*, \end{aligned} \tag{16}$$

where $b = \varepsilon_i\varepsilon_f/q^2$, $a = \left(1 - \left(m_f c^2/\varepsilon_f\right)^2\right)^{1/2}$, and $c = \left(m_f c^2\right)^2/q\varepsilon_f$. In (16), the (−) sign corresponds to neutrino scattering and the (+) sign to antineutrino. The absolute value of the three momentum transfers is given by

$$q = \left|\vec{q}\right| = \sqrt{\omega^2 + 2\varepsilon_f\varepsilon_i\left(1 - a\cos\theta\right) - \left(m_f c^2\right)^2}. \tag{17}$$

For charged current reactions, the cross-sectional equation (14) must be corrected for the distortion of the outgoing lepton wave function by the Coulomb field of the daughter nucleus. The cross section can either be multiplied by the Fermi function $F(\varepsilon_f, Z_f)$ obtained from the numerical solution of the Dirac equation for an extended nuclear charge distribution [29, 63], or, at higher energies, the effect of the Coulomb field can be described by the effective momentum approximation (EMA) [63–65]. In this approximation, the lepton momentum p_f and energy ε_f are modified as

$$\begin{aligned} p_f^{\mathrm{eff}} &= \frac{1}{c}\sqrt{\left(\varepsilon_f^{\mathrm{eff}}\right)^2 - \left(m_f c^2\right)^2} \\ \varepsilon_f^{\mathrm{eff}} &= \varepsilon_f - V_C^{\mathrm{eff}}, \end{aligned} \tag{18}$$

where V_C^{eff} is the effective Coulomb potential. In a recent study using exact Dirac wave functions, it has been shown that an accurate approximation for the effective electron momenta is obtained by using the mean value of the Coulomb potential, $V_C^{\mathrm{eff}} = 4V_C(0)/5$, where $V_C(0) = -3Z_f\alpha/(2R)$ corresponds to the electrostatic potential evaluated at the center of the nucleus [66, 67]. Z_f is the charge of the daughter nucleus, and R is its radius assuming spherical charge distribution. α denotes the fine structure constant. In calculations with EMA, the original lepton momentum p_f and energy ε_f appearing in the expression for the cross section are replaced by the above effective quantities.

3. Energies and Wave Functions

For neutral-current-neutrino-nucleus-induced reactions, the ground state and the excited states of the even-even nucleus are created using the quasiparticle random-phase approximation (QRPA) including two quasineutron and two quasiproton excitations in the QRPA matrix [68] (hereafter denoted by pp-nn QRPA). We start by writing the A-fermion Hamiltonian H, in the occupation-number representation, as a sum of two terms. One is the sum of the single-particle energies (spe) ϵ_α which runs over all values of quantum numbers $\alpha \equiv \{n_\alpha, l_\alpha, j_\alpha, m_\alpha\}$ and the second term which includes the two-body interaction V, that is,

$$H = \sum_\alpha \epsilon_\alpha c_\alpha^\dagger c_\alpha + \frac{1}{4}\sum_{\alpha\beta\gamma\delta} \overline{V}_{\alpha\beta\gamma\delta} c_\alpha^\dagger c_\beta^\dagger c_\delta c_\gamma, \tag{19}$$

where the two-body term contains the antisymmetric two-body interaction matrix element defined by $\overline{V}_{\alpha\beta\gamma\delta} = \langle\alpha\beta|V|\gamma\delta\rangle - \langle\alpha\beta|V|\delta\gamma\rangle$. The operators $c_\alpha^\dagger$ and c_α stand for the usual creation and destruction operators of nucleons in the state α.

For spherical nuclei with partially filled shells, the most important effect of the two-body force is to produce pairing correlations. The pairing interaction is taken into account by using the BCS theory [69]. The simplest way to introduce these correlations in the wave function is to perform the Bogoliubov-Valatin transformation:

$$\begin{aligned} a_\alpha^\dagger &= u_\alpha c_\alpha^\dagger - v_\alpha \widetilde{c}_\alpha, \\ \widetilde{a}_\alpha^\dagger &= u_\alpha \widetilde{c}_\alpha^\dagger + v_\alpha c_\alpha, \end{aligned} \tag{20}$$

where $\widetilde{c}_\alpha^\dagger = c_{-\alpha}^\dagger (-1)^{j_\alpha + m_\alpha}$, $\widetilde{a}_\alpha^\dagger = a_{-\alpha}^\dagger (-1)^{j_\alpha + m_\alpha}$, and $-\alpha \equiv \{n_\alpha, l_\alpha, j_\alpha, -m_\alpha\}$. The occupation amplitudes v_α and u_α are determined via variational procedure for minimizing the energy of the BCS ground state for protons and neutrons, separately. In the BCS approach, the ground state of an even-even nucleus is described as a superconducting medium, where all the nucleons have formed pairs that effectively act as bosons. The BCS ground state is defined as

$$|\mathrm{BCS}\rangle = \prod_{\alpha>0} \left(u_\alpha - v_\alpha c_\alpha^\dagger \widetilde{c}_\alpha^\dagger\right) |\mathrm{CORE}\rangle\ , \tag{21}$$

where $|\mathrm{CORE}\rangle$ represents the nuclear core (effective particle vacuum).

After the transformation (20), the Hamiltonian can be written in its quasiparticle representation as

$$H = \sum_\alpha E_\alpha a_\alpha^\dagger a_\alpha + H_{\mathrm{qp}}, \tag{22}$$

where the first term gives the single-quasiparticle energies E_α, and the second one includes the different components of the residual interaction.

In the present calculations, we use a renormalization parameter g_{pair} which can be adjusted solving the BCS equations. The monopole matrix elements $\langle\alpha\alpha; J=0|V|\beta\beta; J=0\rangle$ of the two-body interaction are multiplied by a factor g_{pair}. The adjustment can be done by comparing the resulting lowest-quasiparticle energy to the phenomenological energy gap Δ obtained from the separation energies of the neighboring doubly even nuclei for protons and neutrons, separately.

The excited states of the even-even reference nucleus are constructed by use of the QRPA. In the QRPA, the creation operator for an excited state $|\omega; J^\pi M\rangle$ has the form

$$\widehat{Q}^\dagger\left(J_\omega^\pi M\right) = \sum_{\alpha\le\alpha'} \left[X_{\alpha\alpha'}^{J_\omega^\pi} A^\dagger\left(\alpha\alpha'; JM\right) - Y_{\alpha\alpha'}^{J_\omega^\pi} \widetilde{A}\left(\alpha\alpha'; JM\right)\right], \tag{23}$$

where the quasiparticle pair creation $A^\dagger(\alpha\alpha'; JM)$ and annihilation $\widetilde{A}(\alpha\alpha'; JM)$ operators are defined as

$$\begin{aligned} A^\dagger\left(\alpha\alpha'; JM\right) &\equiv \left(1+\delta_{\alpha\alpha'}\right)^{-1/2}\left[a_\alpha^\dagger a_{\alpha'}^\dagger\right]_{JM}, \\ \widetilde{A}\left(\alpha\alpha'; JM\right) &\equiv (-1)^{J+M} A\left(\alpha\alpha'; J-M\right), \end{aligned} \tag{24}$$

where α and α' are either proton (p) or neutron (n) indices, M labels the magnetic substates, and ω numbers the states for particular angular momentum J and parity π.

The X and Y forward- and backward-going amplitudes are determined from the QRPA matrix equation

$$\begin{pmatrix} \mathscr{A} & \mathscr{B} \\ -\mathscr{B} & -\mathscr{A} \end{pmatrix} \begin{pmatrix} X^{J^\pi} \\ Y^{J^\pi} \end{pmatrix} = \omega \begin{pmatrix} X^{J^\pi} \\ Y^{J^\pi} \end{pmatrix}, \tag{25}$$

where ω denotes the excitation energies of the nuclear state $|J^\pi\rangle$. The QRPA matrices, $\mathscr{A}$ and $\mathscr{B}$, are deduced by the matrix elements of the double commutators of $A^\dagger$ and A with the nuclear Hamiltonian $\widehat{H}$ defined as

$$\begin{aligned} \mathscr{A}_{\alpha\alpha',\beta\beta'} &= \left\langle \mathrm{BCS}\left|\left[A\left(\alpha\alpha'; JM\right), \widehat{H}, A^\dagger\left(\beta\beta'; JM\right)\right]\right|\mathrm{BCS}\right\rangle, \\ \mathscr{B}_{\alpha\alpha',\beta\beta'} &= -\left\langle \mathrm{BCS}\left|\left[A\left(\alpha\alpha'; JM\right), \widehat{H}, \widetilde{A}\left(\beta\beta'; JM\right)\right]\right|\mathrm{BCS}\right\rangle, \end{aligned} \tag{26}$$

where $2[A,B,C] = [A,[B,C]] + [[A,B],C]$. Finally, the two-body matrix elements of each multipolarity J^π, occurring in the QRPA matrices $\mathscr{A}$ and $\mathscr{B}$, are multiplied by two phenomenological scaling constants, namely, the particle-hole strength g_{ph} and the particle-particle strength g_{pp}. These parameter values are determined by comparing the resulting lowest-phonon energy with the corresponding lowest-collective vibrational excitation of the doubly even nucleus and by reproducing some giant resonances which play crucial role.

For charged current neutrino-nucleus reactions, the excited states $|\omega; J^\pi M\rangle$ of the odd-odd nucleus are generated adopting the proton-neutron QRPA(pnQRPA). The QRPA in its proton-neutron form contains phonons made out of proton-neutron pairs as follows:

$$\widehat{Q}^\dagger\left(J_\omega^\pi M\right) = \sum_{\mathrm{pn}} \left[X_{\mathrm{pn}}^{J_\omega^\pi} A^\dagger\left(\mathrm{pn}; JM\right) - Y_{\mathrm{pn}}^{J_\omega^\pi} \widetilde{A}\left(\mathrm{pn}; JM\right)\right]. \tag{27}$$

The matrices $\mathscr{A}$ and $\mathscr{B}$ defined in the canonical basis are

$$\begin{aligned}\mathscr{A}_{\mathrm{pn,p'n'}} &= \delta_{\mathrm{pn,p'n'}}\left(E_{\mathrm{p}}+E_{\mathrm{n}}\right)\\ &\quad+g_{\mathrm{pp}}\left(u_{\mathrm{p}}u_{\mathrm{n}}u_{\mathrm{p'}}u_{\mathrm{n'}}+v_{\mathrm{p}}v_{\mathrm{n}}v_{\mathrm{p'}}v_{\mathrm{n'}}\right)V^{\mathrm{pp}}_{\mathrm{pn,p'n'}}\\ &\quad+g_{\mathrm{ph}}\left(u_{\mathrm{p}}v_{\mathrm{n}}u_{\mathrm{p'}}v_{\mathrm{n'}}+v_{\mathrm{p}}u_{\mathrm{n}}v_{\mathrm{p'}}u_{\mathrm{n'}}\right)V^{\mathrm{ph}}_{\mathrm{pn,p'n'}},\\ \mathscr{B}_{\mathrm{pn,p'n'}} &= -g_{\mathrm{pp}}\left(u_{\mathrm{p}}u_{\mathrm{n}}v_{\mathrm{p'}}v_{\mathrm{n'}}+v_{\mathrm{p}}v_{\mathrm{n}}u_{\mathrm{p'}}u_{\mathrm{n'}}\right)V^{\mathrm{pp}}_{\mathrm{pn,p'n'}}\\ &\quad+g_{\mathrm{ph}}\left(u_{\mathrm{p}}v_{\mathrm{n}}v_{\mathrm{p'}}u_{\mathrm{n'}}+v_{\mathrm{p}}u_{\mathrm{n}}u_{\mathrm{p'}}v_{\mathrm{n'}}\right)V^{\mathrm{ph}}_{\mathrm{pn,p'n'}},\end{aligned} \tag{28}$$

where E_{p} and E_{n} are the two-quasiparticle excitation energies, and $V^{\mathrm{ph}}_{\mathrm{pn,p'n'}}$ and $V^{\mathrm{pp}}_{\mathrm{pn,p'n'}}$ are the p-h and p-p matrix elements of the residual nucleon-nucleon interaction V, respectively. For charged current reactions, the matrix elements of any transition operator $\mathscr{O}_\lambda$ between the ground state $|0^+_{\mathrm{gs}}\rangle$ and the excited $|\omega; J^\pi M\rangle$ can be factored as follows:

$$\left\langle 0^+_{\mathrm{gs}}\left\|\mathscr{O}_\lambda\right\|\omega; J^\pi M\right\rangle = \sum_{\mathrm{pn}}\langle \mathrm{p}\left\|\mathscr{O}_\lambda\right\|\mathrm{n}\rangle\left(X^{J^\pi}_{\mathrm{pn}}u_{\mathrm{p}}v_{\mathrm{n}}+Y^{J^\pi}_{\mathrm{pn}}v_{\mathrm{p}}u_{\mathrm{n}}\right), \tag{29}$$

where $\langle \mathrm{p}\|\mathscr{O}_\lambda\|\mathrm{n}\rangle$ are the reduced matrix elements calculated independently for a given single-particle basis [70, 71].

4. Results and Discussion

Transition matrix elements of the type entering in (15) and (16) can be calculated in the framework of pnQRPA. The initial nucleus ^{132}Xe was assumed to be spherically symmetric having a 0^+ ground state. Two-oscillator ($3\hbar\omega$ and $4\hbar\omega$) major shells, plus the intruder orbital $h_{11/2}$ from the next higher-oscillator major shell, were used for both protons and neutrons as the valence space of the studied nuclei. The corresponding single-particle energies (SPE) were produced by the Coulomb corrected Woods-Saxon potential using the parameters of Bohr and Mottelson [72].

The two-body interaction matrix elements were obtained from the Bonn one-boson-exchange potential applying G-matrix techniques [73]. The strong pairing interaction between the nucleons can be adjusted by solving the BCS equations. The monopole matrix elements of the two-body interaction are scaled by the pairing-strength parameters $g^{\mathrm{p}}_{\mathrm{pair}}$ and $g^{\mathrm{n}}_{\mathrm{pair}}$, separately, for protons and neutrons. The adjustment can be done by comparing the resulting lowest-quasiparticle energy to reproduce the phenomenological pairing gap [74]. The results of this procedure lead to the pairing-strength parameters $g^{\mathrm{p}}_{\mathrm{pair}} = 0.98$ and $g^{\mathrm{n}}_{\mathrm{pair}} = 1.3$. The particle-particle matrix elements as well as the particle-hole ones are renormalized by means of the parameters g_{pp} and g_{ph}, respectively. These parameters were adjusted for each multipole state separately in order to reproduce few of the experimental known energies of the low-lying states in the ^{132}Cs and ^{132}I nucleus, respectively. The obtained values for the corresponding parameters lie in the range $0.6 \le g_{\mathrm{pp}} \le 1.2$ and $0.5 \le g_{\mathrm{ph}} \le 1.0$. Especially, for the 1^- multipolarity, the values $g_{\mathrm{pp}} = 1.0$ and $g_{\mathrm{ph}} = 0.5$ were used, while for the 1^+ multipolarity, the values $g_{\mathrm{pp}} = 1$ and $g_{\mathrm{ph}} = 1$ were used. Moreover, for ^{132}I, the values $g_{\mathrm{pp}} = 1$ and $g_{\mathrm{ph}} = 1$ were used with the exception of 4^+ multipolarity for which $g_{\mathrm{pp}} = 0.3$ and $g_{\mathrm{ph}} = 1.2$ were used. All the states up to $J = 5^\pm$ have been included.

Table 1: Total cross sections for the indicated neutrino-nucleus charged current reactions as a function of incoming neutrino energy. The cross sections are given in units of 10^{-42} cm^2, and exponents are given in parentheses.

E_ν (MeV)	ν-^{132}Xe	$\bar{\nu}$-^{132}Xe
7.0	5.37 (−2)	2.05 (−4)
10.0	2.09 (+1)	1.63 (−1)
15.0	1.97 (+2)	2.46 (0)
20.0	6.27 (+2)	1.75 (+1)
25.0	1.30 (+3)	4.75 (+1)
30.0	1.82 (+3)	8.69 (+1)
40.0	2.76 (+3)	1.77 (+2)
50.0	3.74 (+3)	3.93 (+2)
60.0	4.76 (+3)	6.92 (+2)
70.0	5.75 (+3)	9.83 (+2)
80.0	6.63 (+3)	1.24 (+3)
90.0	7.32 (+3)	1.47 (+3)
100.0	7.78 (+3)	1.69 (+3)

Table 2: Flux-averaged cross sections (10^{-40} cm^2) obtained by convoluting the cross sections of Figure 3 with (3). Different temperatures T (MeV) and α values are considered. The average neutrino energy $\langle E_\nu\rangle$ is given in MeV.

(T, α)	$\langle E_\nu\rangle$	ν_e − CC	$\bar{\nu}_e$ − CC
(3.5, 0)	11.0	1.74	0.05
(4, 0)	12.6	2.65	0.09
(5, 0)	15.7	4.90	0.21
(6, 0)	20.0	7.52	0.40
(8, 0)	25.2	13.27	0.95
(10, 0)	31.5	19.05	1.73
(2.75, 3)	11.0	1.31	0.03
(3.5, 3)	14.0	3.03	0.09
(4, 3)	16.0	4.52	0.17
(5, 3)	20.0	8.00	0.37
(6, 3)	24.0	11.83	0.67
(8, 3)	32.0	19.62	1.58
(10, 3)	40.0	26.95	2.80

Table 3: Expected event rates for a 3 kT xenon detector for a supernova at 10 kpc corresponding to $\langle E_{\nu_e}\rangle = 11$ MeV and $\langle E_{\bar{\nu}_e}\rangle = 16$ MeV.

	^{132}Xe$(\nu_e, e^-)^{132}$Cs*	^{132}Xe$(\bar{\nu}_e, e^+)^{132}$I*	Total event rates
$\alpha = 0$	592	50	642
$\alpha = 3$	445	40	485

Table 4: Fraction (in %) of the flux-averaged cross section associated to states of a given multipolarity with respect to the total flux-averaged cross section, that is, $\langle\sigma\rangle_{J^\pi}/\langle\sigma\rangle_{\text{tot}}$. The first column tells if the results correspond to low-energy beta-beams or to a conventional source (DAR is for the decay at rest of muons). The neutrino fluxes are those produced by boosted ^{18}Ne ions. The Lorentz ion boost parameter γ takes the values 6, 10, and 14. The last column gives the total flux-averaged cross sections (10^{-40} cm^2).

	0^+	1^+	2^+	3^+	4^+	0^-	1^-	2^-	3^-	4^-	$\langle\sigma\rangle$ (10^{-40} cm^2)
$\gamma = 6$	13.3	69.4	1.45	0.47	0.004	0.00002	10.52	4.23	0.19	0.10	8.17
10	14.4	49.8	5.54	1.96	0.08	0.00002	19.0	6.58	1.66	0.90	19.14
14	13.1	37.9	9.40	3.56	0.46	0.00002	20.7	7.09	5.05	2.67	29.46
DAR	14.9	52.6	4.45	1.54	0.03	0.00002	18.4	6.42	1.02	0.55	19.47

Table 5: Same as Table 4, but for the antineutrino-nucleus cross sections and the antineutrino fluxes produced by boosted ^{6}He ions.

	0^+	1^+	2^+	3^+	4^+	0^-	1^-	2^-	3^-	4^-	$\langle\sigma\rangle$ (10^{-40} cm^2)
$\gamma = 6$	32.0	53.8	0.76	0.18	0.0007	0.00003	9.05	4.12	0.07	0.04	0.37
10	34.4	44.3	2.00	0.51	0.008	0.00004	12.88	5.28	0.34	0.21	1.57
14	33.6	38.1	3.54	1.18	0.06	0.00002	15.17	6.25	1.12	0.91	3.69

In Figure 1, we present the numerical results of the total scattering cross section $\sigma(E_\nu)$ (14) as a function of the incoming neutrino energy E_ν for the reactions $^{132}\text{Xe}(\nu_e, e^-)^{132}\text{Cs}$ and $^{132}\text{Xe}(\overline{\nu}_e, e^+)^{132}\text{I}$, respectively. The Q values of the reactions are 2.12 MeV and 3.58 MeV, respectively. Here, we have considered a hybrid prescription already used in previous calculations [19, 75, 76], where the Fermi function for the Coulomb correction is used below the energy region on which both approaches predict the same values, while EMA is adopted above this energy region.

The contribution of the different multipoles to the total cross section for the impinging neutrino energies $E_{\nu_e} = 20, 60$, and 80 MeV is shown in Figure 2. When $E_{\nu_e} = 20$ MeV, the total cross section σ_{ν_e} is mainly ascribed to the Gamow-Teller (1^+) and the Fermi (0^+) transitions. Other transitions contribute only a few percent to the total cross section. As the neutrino energy increases, the multipole states $J^\pi = 1^-, 2^-$, and 2^+ become important as well. Finally, beyond 80 MeV, all states contribute, and the cross section is being spread over many multipoles.

Figure 3 shows the cross sections of coherent neutral and charged current processes as a function of neutrino energy. As it is seen, the coherent neutral current (ν − NC) process [55] presents cross sections which are an order of magnitude greater than the electron neutrino charged current cross sections (ν_e − CC). Both of them are even bigger than those from electron antineutrino charge current cross section ($\overline{\nu}_e$ − CC) events. At $E_\nu = 80$ MeV, the difference between ν_e − CC and $\overline{\nu}_e$ − CC turns out to be a factor of 5. This can be understood in terms of the energy threshold and nuclear effects of the reactions. Since the Q value for the $\overline{\nu}_e$ reactions is 1.46 MeV greater than ν_e one, it decreases the incident neutrino energy as $E_\nu \to E_\nu - Q$ and therefore reduces the $\overline{\nu}_e$ cross section for a given energy. In Table 1, the total (anti-) neutrino cross sections are listed in units of 10^{-42} cm^2.

The flux-averaged total cross sections $\langle\sigma\rangle$ can be calculated by folding the cross sections shown in Figure 3 with the Fermi-Dirac spectrum given by (3) as follows:

$$\langle\sigma\rangle = \int_0^\infty \sigma(E_\nu)\,\phi(E_\nu)\,dE_\nu. \tag{30}$$

Table 2 shows the flux-averaged total cross sections for different values of temperature T. The chemical potential parameters $\alpha = 0$ and $\alpha = 3$ have been used in order to describe the supernova spectrum [32]. The corresponding average neutrino energy $\langle E_\nu\rangle$ has been calculated by means of (4) and (5). As it is seen, the calculated flux-averaged cross section increases as the average neutrino energy increases. The introduction of a chemical potential in the spectrum at fixed neutrino temperature increases the average neutrino energy. In Figure 4, a contour plot is used to display lines of constant flux-averaged cross sections (in units of 10^{-39} cm^2) of $^{132}\text{Xe}(\nu_e, e^-)^{132}\text{Cs}^*$ reaction, as a function of T and α. At lower temperatures, the flux-averaged cross sections depend only very weakly on α. However, already above $T = 2$ MeV, the flux-averaged cross sections increase much faster for higher values of the chemical potential α.

In Table 3, we present the number of expected events for supernova explosion occurring at a distance of 10 kpc from earth, releasing an energy of 3×10^{53} ergs. These event rate calculations have been done for 3 kT Xenon detector corresponding to various values of temperature T with $\alpha = 0$ and 3. Using $\alpha = 3$, we find the total event rate of 485 which corresponds to a decrease of 32% as compared to the $\alpha = 0$ supernova neutrino spectrum.

In the literature, there are suggestions to look for charged current neutrino-nucleus scattering at several neutrino sources. We propose to look for this reaction with a terrestrial neutrino sources with spectra similar to those of SN neutrinos, using a near detector whose active target consists of a noble liquid gas such as ^{132}Xe. In this paper, we examine two possibilities: (i) the low-energy neutrino spectra corresponding to conventional neutrino sources, that is, muon decay at rest (DAR) given by the well-known Michel

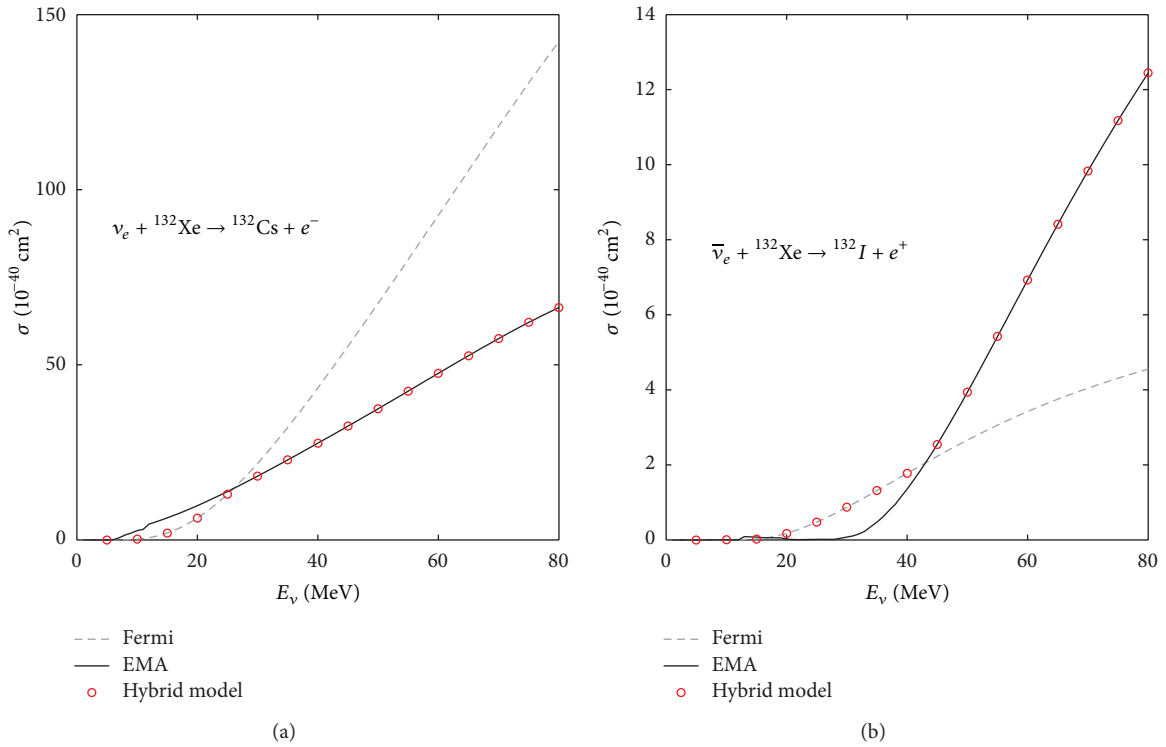

FIGURE 1: (Color on line). Total cross section as a function of the incoming neutrino energy E_ν, in the CC reactions $^{132}\mathrm{Xe}(\nu_e, e^-)^{132}\mathrm{Cs}$ (a) and $^{132}\mathrm{Xe}(\bar{\nu}_e, e^+)^{132}\mathrm{I}$ (b).

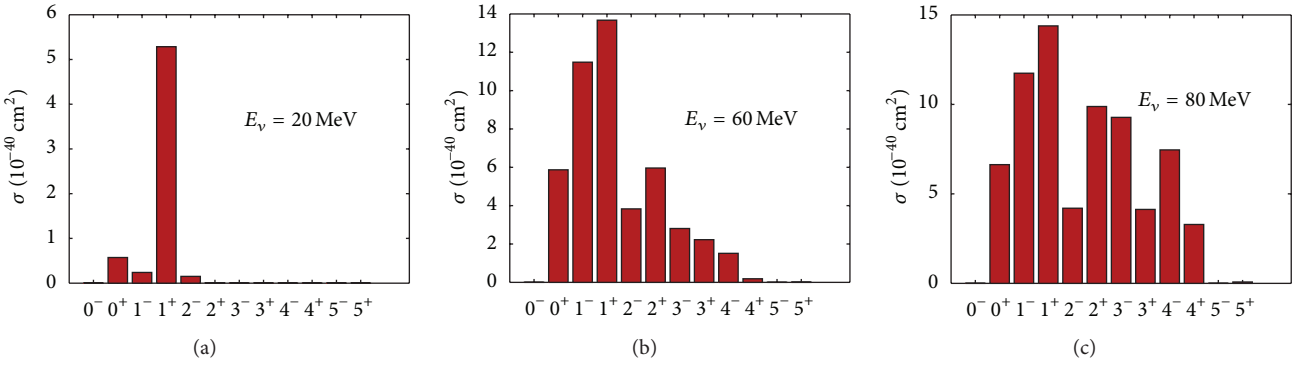

FIGURE 2: (Color on line). Partial multipole distributions to the total cross sections for $^{132}\mathrm{Xe}(\nu_e, e^-)^{132}\mathrm{Cs}$, at the incoming neutrino energies E_ν = 20, 60, and 80 MeV.

spectrum from muons decaying at rest and (ii) the low-energy beta-beams with a boosted parameter γ.

Several experiments to be done at low-energy beta-beam have been proposed. Throughout our calculations, we have assumed that the boosted ions are storage in a ring similar to that used in [77]. Its total length is $L = 450$ m with straight section length 150 m, while the detector is located 10 m away from the straight section. The radius of the cylindrical detector is 2.13 m with thickness 5 m. As seen in Figure 5, the DAR spectrum has quite similar shape to the low-energy beta-beam spectrum with $\gamma = 10$. Note that, in principle, since the cross sections approximately grow as the neutrino energy square, the flux-averaged cross sections can show differences due to the high energy part of the neutrino spectrum.

Table 4 presents the contribution of the different states to the flux-averaged cross section. One can see that the results for $\gamma = 10$ are similar to the DAR case. The neutrino-Xenon cross section is dominated by the $0^+, 1^+$, and 1^- multipoles. When the ion boost parameter γ increases, the relative contribution of the 1^+ decreases in favor of all other multipoles except 0^+ which seems to be almost constant. For $\gamma = 14$, the contribution of all states becomes important in agreement with previously published results [76]. Table 5 presents the results for the antineutrino scattering, where the antineutrino fluxes are produced by the decay of boosted

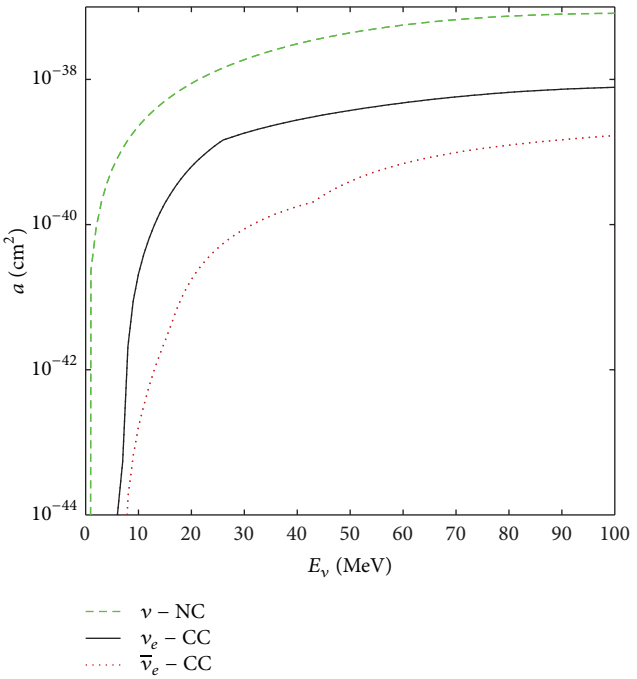

Figure 3: (Color on line). Comparison of cross sections for relevant neutrino reactions on ^{132}Xe.

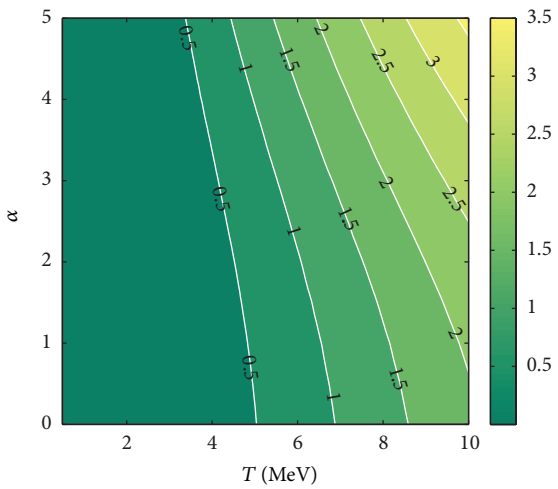

Figure 4: (Color online). Contour plot of supernova neutrino-nucleus flux-averaged cross sections (in units of 10^{-39} cm^2) for the ^{132}Xe$(\nu_e, e^-)^{132}$Cs* reaction as functions of the temperature T and chemical potential α, that determine the Fermi-Dirac neutrino spectrum. The solid lines in the plot correspond to constant values of flux-averaged cross section. The lighter shading area denotes the increase of flux-averaged cross sections.

^{6}He ions. As it can be seen, the contribution of both 0^+ and 1^+ transitions to the flux-averaged cross sections is lying between 86% for boosted ions at $\gamma = 6$ and 72% for $\gamma = 14$.

5. Conclusions

Detailed microscopic calculations of charged current and neutral current neutrino-nucleus reaction rates are of crucial importance for models of neutrino oscillations, detection of supernova neutrinos, and studies of the r-process nucleosynthesis. In this paper we have calculated charged-current-neutrino-induced reactions on ^{132}Xe by including multipole transitions up to $J = 5^{\pm}$. Excited states up to a few tens of MeV are taken into account. The ground state of ^{132}Xe is described with the BCS model, and the neutrino-induced transitions to excited nuclear states are computed in the quasiparticle random-phase approximation.

In addition to the total neutrino-nucleus cross sections, we have also analyzed the evolution of the contributions of different multipole excitations as a function of neutrino energy. It has been shown that except at relatively low-neutrino energies $E_\nu \leq 30$ MeV for which the reactions are dominated by the transitions to 0^+ and 1^+ states, at higher energies, the inclusion of spin-dipole transitions, as well as excitations of higher multipolarities, is essential for a quantitative description of neutrino-nucleus cross sections. It is found that the ν_e cross section on ^{132}Xe is about 5 times greater than the $\overline{\nu}_e$ one. This difference is anticipated because of (i) the different Q values of the corresponding reactions, (ii) the fact that there are less excited states that one can populate in the $\overline{\nu}_e$ channel with respect to the ν_e one and (iii) the different sign (minus for neutrino plus for antineutrino) of the interference term of magnetic and electric transitions introduced in (16).

Finally, we have given the contribution of the different states to the flux-averaged cross section considering low energy neutrino beams.

These are either based on conventional sources (muon decay at rest) or on low-energy beta-beams. We found that the Gamow-Teller (1^+) and the Fermi (0^+) transitions are the main components. When the Lorentz ion boost parameter γ

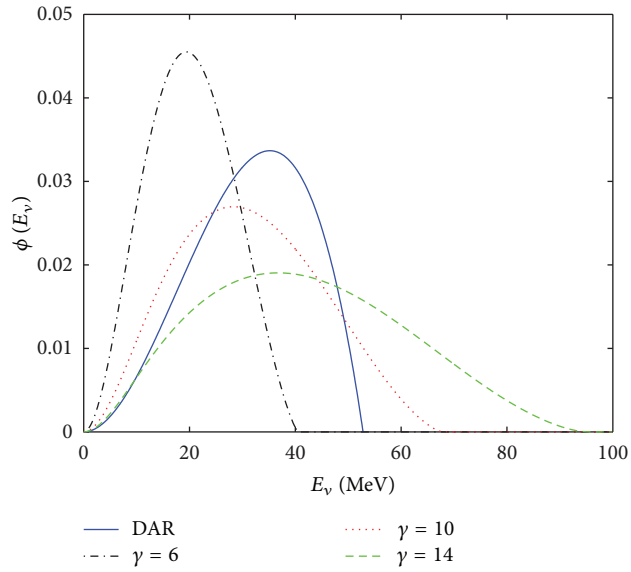

Figure 5: Normalized neutrino spectra stemming from the decay of ^{18}Ne ions boosted at $\gamma = 6$ (dot-dashed line), $\gamma = 10$ (dotted line) and $\gamma = 14$ (dashed line). The full line presents the Michel spectrum for neutrinos from muon decay-at-rest.

increases, the relative contribution of 1^+ decreases in favor of all other multipole states except 0^+ which seems to be almost constant, while the contribution of other states like 1^-, 2^-, 2^+, 3^-, and 3^+ become important as well.

References

[1] T. W. Donnelly and R. D. Peccei, "Neutral current effects in nuclei," *Physics Reports*, vol. 50, no. 1, pp. 1–85, 1979.

[2] R. Davis, "A review of the homestake solar neutrino experiment," *Progress in Particle and Nuclear Physics*, vol. 32, pp. 13–32, 1994.

[3] K. Langanke, "Weak interaction, nuclear physics and supernovae," *Acta Physica Polonica B*, vol. 39, pp. 265–282, 2008.

[4] W. C. Haxton, "Radiochemical neutrino detection via $^{127}\mathrm{I}(V_e, e^-)^{127}\mathrm{Xe}$," *Physical Review Letters*, vol. 60, no. 9, pp. 768–771, 1988.

[5] J. N. Bahcall and R. K. Ulrich, "Solar models, neutrino experiments, and helioseismology," *Reviews of Modern Physics*, vol. 60, no. 2, pp. 297–372, 1988.

[6] K. Kubodera and S. Nozawa, "Neutrino-nucleus reactions," *International Journal of Modern Physics E*, vol. 3, no. 1, pp. 101–148, 1994.

[7] J. Rapaport et al., "Empirical Evaluation of Gamow-Teller Strength Function for $^{37}\mathrm{Cl} \rightarrow {}^{37}\mathrm{Ar}$ and its Implication in the Cross Section for Solar Neutrino Absorption by $^{37}\mathrm{Cl}$," *Physical Review Letters*, vol. 47, no. 21, pp. 1518–1521, 1981.

[8] J. Rapaport, P. Welch, J. Bahcall et al., "Solar-neutrino detection: experimental determination of gamow-teller strengths via the $^{98}\mathrm{Mo}$ and $^{115}\mathrm{In}$ $(p, 2)$ Reactions," *Physical Review Letters*, vol. 54, no. 21, pp. 2325–2328, 1985.

[9] D. Krofcheck et al., "Gamow-teller strength function in $^{71}\mathrm{Ge}$ via the $(p, 2)$ reaction at medium energies," *Physical Review Letters*, vol. 55, no. 10, p. 1051, 1985.

[10] D. Krofcheck, E. Sugarbaker, A.J. Wagner et al., "Gamow-Teller strength distribution in $^{81}\mathrm{Kr}$ and the consequences for a $^{81}\mathrm{Br}$ solar neutrino detector," *Physics Letters B*, vol. 189, no. 3, pp. 299–303, 1987.

[11] S. Yu. Lutostansky and N. B. Skulgina, "Strength function of $^{127}\mathrm{Xe}$ and iodine-xenon neutrino detector," *Physical Review Letters*, vol. 67, no. 4, p. 430, 1991.

[12] "Scientific opportunities at the oak ridge laboratory for neutrino detectors (ORLAND)," in *Workshop on Neutrino Nucleus Physics Using a Stopped Pion Neutrino Facility*, pp. 22–26, Tennessee, Oak Ridge, Tenn, USA, May 2000.

[13] S. Freedman, B. Kayser et al., "The neutrino matrix: DNP/DPF/DAP/DPB joint study on the future of neutrino physics," Tech. Rep., American Physical Society, 2004.

[14] J. A. Formaggio and G. P. Zeller, "From eV to EeV: neutrino cross sections across energy scales," *Reviews of Modern Physics*, vol. 84, no. 3, pp. 1307–1341, 2012.

[15] R. Maschuw, "KARMEN collaboration," *Progress in Particle and Nuclear Physics*, vol. 40, pp. 183–192, 1998.

[16] M. Albert, C. Athanassopoulos, L. B. Auerbach et al., "Measurement of the reaction $^{12}\mathrm{C}$(nu micro, micro-)X near threshold," *Physical Review*, vol. 51, pp. R1065–R1069, 1995.

[17] S. P. Riley et al., "Neutrino-induced deuteron disintegration experiment," *Physical Review C*, vol. 59, no. 3, pp. 1780–1789, 1999.

[18] A. C. Hayes, "Nuclear structure issues determining neutrino-nucleus cross sections," *Physics Reports*, vol. 315, no. 1–3, pp. 257–271, 1999.

[19] C. Volpe, N. Auebach, G. Colo, T. Suzuki, and N. Van Giai, "Microscopic theories of neutrino-$^{12}\mathrm{C}$ reactions," *Physical Review C*, vol. 62, no. 1, Article ID 015501, 11 pages, 2000.

[20] N. Paar, D. Vretenar, and T. Marketin, "Inclusive charged-current neutrino-nucleus reactions calculated with the relativistic quasiparticle random-phase approximation," *Physical Review C*, vol. 77, no. 2, Article ID 024608, 11 pages, 2008.

[21] M. K. Cheoum, E. Ha, T. Hayakawa, T. Kajino, and S. Chiba, "Neutrino reactions on $^{138}\mathrm{La}$ and $^{180}\mathrm{Ta}$ via charged and neutral currents by the quasiparticle random-phase approximation," *Physical Review C*, vol. 82, no. 3, Article ID 035504, 7 pages, 2010.

[22] N. Jachowicz, K. Heyde, J. Ryckebusch, and S. Rombouts, "Continuum random phase approximation approach to charged-current neutrino-nucleus scattering," *Physical Review C*, vol. 65, no. 2, Article ID 025501, 7 pages, 2002.

[23] V. Tsakstara, T. S. Kosmas, P. C. Divari, and J. Sinatkas, "Supernova neutrino detection by terrestrial nuclear detectors," *Progress in Particle and Nuclear Physics*, vol. 64, no. 2, pp. 411–413, 2010.

[24] P. C. Divari, V. C. Chasioti, and T. S. Kosmas, " Neutral current neutrino-$^{98}\mathrm{Mo}$ reaction cross sections at low and intermediate energies," *Physica Scripta*, vol. 82, no. 6, Article ID 065201, 2010.

[25] V. Tsakstara and T. S. Kosmas, "Low-energy neutral-current neutrino scattering on $^{128,130}\mathrm{Te}$ isotopes," *Physical Review Letters C*, vol. 83, no. 5, Article ID 054612, 13 pages, 2011.

[26] V. C. Chasioti, T. S. Kosmas, and P. C. Divari, "Inelastic neutrino-nucleus reaction cross sections at low neutrino-energies," *Progress in Particle and Nuclear Physics*, vol. 59, no. 1, pp. 481–485, 2007.

[27] F. Krmpotic, A. Mariano, and A. Samana, "Neutrino-nucleus reactions and muon capture in $^{12}\mathrm{C}$," *Physical Review C*, vol. 71, no. 4, Article ID 044319, 14 pages, 2005.

[28] E. Kolbe, K. Langanke, and P. Vogel, "Weak reactions on $^{12}\mathrm{C}$ within the continuum random phase approximation with partial occupancies," *Nuclear Physics A*, vol. 652, no. 1, pp. 91–100, 1999.

[29] E. Kolbe, K. Langanke, G. Martinez-Pinedo, and P. Vogel, "Neutrino-nucleus reactions and nuclear structure," *Journal of Physics G*, vol. 29, no. 11, p. 2569, 2003.

[30] T. Kuramoto, M. Fukugita, Y. Kohyama, and K. Kubodera, "Neutrino-induced reaction cross sections at intermediate energies for chlorine and water detectors," *Nuclear Physics A*, vol. 512, no. 4, pp. 711–736, 1990.

[31] D. S. Miller, J. R. Wilson, and R. W. Mayle, "Convection above the neutrinosphere in type II supernovae," *The Astrophysical Journal*, vol. 415, no. 1, pp. 278–285, 1993.

[32] H. T. Janka and W. Hillebrandt, "Neutrino emission from type II supernovae—an analysis of the spectra," *Astronomy & Astrophysics*, vol. 224, no. 1-2, pp. 49–56, 1989.

[33] M. S. Athar, S. Ahmad, and S. K. Singh, "Supernova neutrino induced inclusive reactions on $^{56}\mathrm{Fe}$ in terrestrial detectors," *Physical Review C*, vol. 71, no. 4, Article ID 045501, 7 pages, 2005.

[34] M. Th. Keil, G. G. Rafelt, and H. -T Janka, "Monte carlo study of supernova neutrino spectra formation," *The Astrophysical Journal*, vol. 590, no. 2, p. 971, 2003.

[35] L. Hudephol, B. Muller, H. T. Janka, A. Marek, and G. G. Raelt, "Neutrino signal of electron-capture supernovae from core collapse to cooling," *Physical Review Letters*, vol. 104, no. 25, Article ID 251101, 4 pages, 2010.

[36] T. Fischer, S. C. Whitehouse, A. Mezzacappa, F. K. Thielemann, and M. Liebendorfer, "Protoneutron star evolution and the neutrino-driven wind in general relativistic neutrino radiation hydrodynamics simulations," *Astronomy & Astrophysics*, vol. 517, no. A80, 2010.

[37] P. C. Divari, S. Galanopoulos, and G. A. Souliotis, "Coherent scattering of neutral-current neutrinos as a probe for supernova detection," *Journal of Physics G*, vol. 39, no. 9, Article ID 095204, 2012.

[38] F. T. Avignone and Y. V. Efremenko J, "Neutrino-nucleus cross-section measurements at intense, pulsed spallation sources," *Journal of Physics G*, vol. 29, no. 11, p. 2615, 2003.

[39] P. Zucchelli, "A novel concept for a $\overline{V}e/Ve$ neutrino factory: the β-beam," *Physics Letters B*, vol. 532, no. 3-4, pp. 166–172, 2002.

[40] C. Volpe, "What about a β-beam facility for low-energy neutrinos?" *Journal of Physics G*, vol. 30, no. 7, 2004.

[41] J. Serreau and C. Volpe, "Neutrino-nucleus interaction rates at a low-energy β-beam facility," *Physical Review C*, vol. 70, no. 5, Article ID 055502, 6 pages, 2004.

[42] G. C. McLaughlin, "Neutrino-lead cross section measurements using stopped pions and low energy β beams," *Physical Review C*, vol. 70, no. 4, Article ID 045804, 5 pages, 2004.

[43] N. Jachowicz and G. C. McLaughlin, "Reconstructing supernova-neutrino spectra using low-energy β beams," *Physical Review Letters*, vol. 96, no. 17, Article ID 172301, 4 pages, 2006.

[44] G. C. McLaughlin and C. Volpe, "Prospects for detecting a neutrino magnetic moment with a tritium source and β-beams," *Physics Letters B*, vol. 591, no. 3-4, pp. 229–234, 2004.

[45] A. B. Balantekin, J. H. de Jesus, and C. Volpe, "Electroweak tests at β-beams," *Physics Letters B*, vol. 634, no. 2-3, pp. 180–184, 2006.

[46] A. B. Balantekin, J. H. de Jesus, R. Lazauskas, and C. Volpe, "Conserved vector current test using low energy β beams," *Physical Review D*, vol. 73, no. 7, Article ID 073011, 2006.

[47] A. Bueno, M. C. Carmona, J. Lozano, and S. Navas, "Observation of coherent neutrino-nucleus elastic scattering at a β beam," *Physical Review D*, vol. 74, no. 3, Article ID 033010, 6 pages, 2006.

[48] J. Barranco, O. G. Miranda, and T. I. Rashba, "Sensitivity of low energy neutrino experiments to physics beyond the standard model," *Physical Review D*, vol. 76, no. 7, 9 pages.

[49] C. Volpe, "Beta-beams," *Journal of Physics G*, vol. 34, no. 1, p. R1, 2007.

[50] S. Amerio, S. Amorusob, and M. Antonelloc, "Design, construction and tests of the ICARUS T600 detector," *Nuclear Instruments and Methods in Physics Research Section A*, vol. 527, no. 3, pp. 329–410, 2004.

[51] E. Aprile et al., "The XENON dark matter search experiment," *New Astronomy Reviews*, vol. 49, no. 2-3, pp. 289–295, 2005.

[52] T. Sumner (UKDMC Collaboration), in *Proceedings of Science (HEP '05)*, 2006, 003.

[53] K. Langanke, "Weak interaction, nuclear physics and supernovae," *Acta Physica Polonica B*, vol. 39, no. 2, pp. 265–281, 2008.

[54] S. Aune, P. Colas, J. Dolbeau et al., "NOSTOS: a spherical TPC to detect low energy neutrinos," *AIP Conference Proceedings*, vol. 785, pp. 110–118, 2005.

[55] P. C. Divari, "Coherent and incoherent neutral current scattering for supernova detection," *Advances in High Energy Physics*, vol. 2012, Article ID 379460, 18 pages, 2012.

[56] Y. Giomataris and J. D. Vergados, "A network of neutral current spherical TPCs for dedicated supernova detection," *Physics Letters B*, vol. 634, no. 1, pp. 23–29, 2006.

[57] I. Giomataris, I. Irastorza, I. Savvidis et al., "A novel large-volume spherical detector with proportional amplification read-out," *Journal of Instrumentation*, vol. 3, Article ID P09007, 2008.

[58] T. Dafni, E. Ferrer-Ribas, I. Giomataris et al., "Energy resolution of alpha particles in a microbulk Micromegas detector at high pressure argon and xenon mixtures," *Nuclear Instruments and Methods in Physics Research Section A*, vol. 608, no. 2, pp. 259–266, 2009.

[59] M. S. Athar, S. Ahmad, and S. K. Singh, "Neutrino nucleus cross sections for low energy neutrinos at SNS facilities," *Nuclear Physics A*, vol. 764, pp. 551–568, 2006.

[60] S. K. Singh, "Electroweak form factors," *Nuclear Physics B*, vol. 112, no. 1–3, pp. 77–85, 2002.

[61] A. Meucci, C. Giusti, and F. D. Pacati, "Neutral-current neutrino-nucleus quasielastic scattering," *Nuclear Physics A*, vol. 744, pp. 307–322, 2004.

[62] T. W. Donnelly and J. D. Walecka, "Elastic magnetic electron scattering and nuclear moments," *Nuclear Physics A*, vol. 201, no. 1, pp. 81–106, 1973.

[63] J. Engel, "Approximate treatment of lepton distortion in charged-current neutrino scattering from nuclei," *Physical Review C*, vol. 57, no. 4, pp. 2004–2009, 1998.

[64] M. Traini, "Coulomb distortion in quasielastic (e,e') scattering on nuclei: Effective momentum approximation and beyond," *Nuclear Physics A*, vol. 694, no. 1-2, p. 325, 2001.

[65] A. Aste and J. Jourdan, "Improved effective momentum approximation for quasielastic (e,e') scattering off highly charged nuclei," *Europhysics Letters*, vol. 67, no. 5, p. 753, 2004.

[66] A. Aste, C. von Arx, and D. Trautmann, "Coulomb distortion of relativistic electrons in the nuclear electrostatic field," *The European Physical Journal A*, vol. 26, no. 2, pp. 167–178, 2005.

[67] A. Aste and D. Trautmann, "Focusing of high-energy particles in the electrostatic field of a homogeneously charged sphere and the effective momentum approximatio," *European Physical Journal A*, vol. 33, no. 11, 16 pages, 2007.

[68] P. Ring and P. Schuck, *The Nuclear Many-Body Problem*, Springer, New York, NY, USA, 1980.

[69] A. Bohr, B. R. Mottelson, and D. Pines, "Possible analogy between the excitation spectra of nuclei and those of the superconducting metallic state," *Physical Review*, vol. 110, no. 4, pp. 936–938, 1958.

[70] T. W. Donnelly and W. C. Haxton, "Multipole operators in semileptonic weak and electromagnetic interactions with nuclei: harmonic oscillator single-particle matrix elements," *Atomic Data and Nuclear Data Tables*, vol. 23, no. 2, pp. 103–176, 1979.

[71] V. Ch. Chasioti and T. S. Kosmas, "A unified formalism for the basic nuclear matrix elements in semi-leptonic processes," *Nuclear Physics A*, vol. 829, pp. 234–252, 2009.

[72] A. Bohr and B. R. Mottelson, *Nuclear Structure*, vol. 1, Benjamin, New York, NY, USA, 1969.

[73] K. Holinde, "Two-nucleon forces and nuclear matter," *Physics Reports*, vol. 68, no. 3, pp. 121–188, 1981.

[74] G. Audi et al., "Cumulative author index volumes A701-A717," *Nuclear Physics A*, vol. 717, no. 3-4, pp. 337–369, 2003.

[75] M. S. Athar, S. Ahmad, and S. K. Singh, "$Ve(\overline{V}e)$–^{40}Ar absorption cross sections for supernova neutrinos," *Physics Letters B*, vol. 591, no. 1-2, pp. 69–75, 2004.

[76] R. Lazauskas and C. Volpe, "Neutrino beams as a probe of the nuclear isospin and spin-isospin excitations," *Nuclear Physics A*, vol. 792, no. 3-4, pp. 219–228, 2007.

[77] P. S. Amanik and G. C. McLaughlin, "Manipulating a neutrino spectrum to maximize the physics potential from a low energy β beam," *Physical Review C*, vol. 75, Article ID 065502, 18 pages, 2007.